



Contents lists available at ScienceDirect

Lung Cancer

journal homepage: www.elsevier.com/locate/lungcan



MET gene exon 14 deletion created using the CRISPR/Cas9 system enhances cellular growth and sensitivity to a *MET* inhibitor

Yosuke Togashi^a, Hiroshi Mizuuchi^b, Shuta Tomida^a, Masato Terashima^a,
Hidetoshi Hayashi^a, Kazuto Nishio^{a,*}, Tetsuya Mitsudomi^b

^a Department of Genome Biology, Kinki University Faculty of Medicine, Japan

^b Department of Thoracic Surgery, Kinki University Faculty of Medicine, Japan

ARTICLE INFO

Article history:

Received 26 July 2015

Received in revised form 21 October 2015

Accepted 22 October 2015

Keywords:

MET exon 14 deletion

CRISPR/Cas9

Crizotinib

Lung adenocarcinoma

ABSTRACT

Background: *MET* splice site mutations resulting in an exon 14 deletion have been reported to be present in about 3% of all lung adenocarcinomas. Patients with lung adenocarcinoma and a *MET* splice site mutation who have responded to *MET* inhibitors have been reported. The CRISPR/Cas9 system is a recently developed genome-engineering tool that can easily and rapidly cause small insertions or deletions.

Materials and methods: We created an *in vitro* model for *MET* exon 14 deletion using the CRISPR/Cas9 system and the HEK293 cell line. The phenotype, which included *MET* inhibitor sensitivity, was then investigated *in vitro*. Additionally, *MET* splice site mutations were analyzed in several cancers included in The Cancer Genome Atlas (TCGA) dataset.

Results: An HEK293 cell line with a *MET* exon 14 deletion was easily and rapidly created; this cell line had a higher *MET* protein expression level, enhanced *MET* phosphorylation, and prolonged *MET* activation. In addition, a direct comparison of phenotypes using this system demonstrated enhanced cellular growth, colony formation, and *MET* inhibitor sensitivity. In the TCGA dataset, lung adenocarcinomas had the highest incidence of *MET* exon 14 deletions, while other cancers rarely carried such mutations. Approximately 10% of the lung adenocarcinoma samples without any of driver gene alterations carried the *MET* exon 14 deletion.

Conclusions: These findings suggested that this system may be useful for experiments requiring the creation of specific mutations, and the present experimental findings encourage the development of *MET*-targeted therapy against lung cancer carrying the *MET* exon 14 deletion.

© 2015 Elsevier Ireland Ltd. All rights reserved.

1. Introduction

Lung cancer is the leading cause of cancer-related mortality worldwide, and approximately 80% of lung cancers are classified as non-small-cell lung cancer (NSCLC) [1]. The identification of epidermal growth factor receptor gene mutations (*EGFR* mutations) as oncogenic driver mutations in a subset of patients with NSCLC, coupled with the development of *EGFR* tyrosine kinase inhibitors, has opened the door to a new era in the treatment of this disease [2–7]. Although the most prevalent mutated or rearranged oncogenes identified in NSCLC are *EGFR*, *KRAS*, *ALK*, *RET*, and *ROS1*, a

subset of unknown alterations seems to persist, and the further identification of new molecular targets is required [8].

MET is a receptor tyrosine kinase (RTK) that was first characterized as a protooncogene in 1984 in a chemically transformed osteosarcoma cell line [9]. The natural ligand for *MET* is hepatocyte growth factor (HGF), also known as scatter factor [10]. After HGF binding, *MET* undergoes dimerization and phosphorylation, which in turn promotes the recruitment of downstream effector proteins leading to the activation of multiple signal cascades, including the MAPK, PI3K/AKT, STAT, and NF- κ B pathways [11]. The aberrant activation of *MET* promotes oncogenicity in a subset of several malignancies including lung adenocarcinoma, gastric cancer, and so on [12–14]. A variety of mechanisms can activate the *MET* signal, including *MET* gene amplification, protein overexpression, activating point mutations, and the induction of its ligand HGF [11,15]. Previous studies have demonstrated that a *MET* splice site mutation that results in an exon 14 deletion induces *MET* activity and may be associated with the sensitivity to *MET* inhibi-

* Corresponding author at: Department of Genome Biology, Kinki University Faculty of Medicine, 377-2 Ohno-higashi, Osaka-Sayama, Osaka 589-8511, Japan. Fax: +81 72 367 6369.

E-mail address: knishio@med.kindai.ac.jp (K. Nishio).

tion [16,17], and we previously reported that about 3% of all lung adenocarcinomas carry this mutation exclusively of other known driver mutations (*EGFR*, *HER2*, and *KRAS*) [18]. Indeed, frequent *MET* splice site mutations have been recently described in whole exome sequencing discovery efforts in lung adenocarcinoma [19]. Crizotinib, a multitargeted tyrosine kinase inhibitor that has activity in *ALK*- or *ROS1*-rearranged lung adenocarcinoma [20,21], was initially designed as a *MET* inhibitor [22], and patients with lung adenocarcinoma and a *MET* splice site mutation who responded to crizotinib have been reported [17,23,24].

The CRISPR/Cas9 (clustered regularly interspaced short palindromic repeat/CRISPR-associated 9) system is a recently developed genome-engineering tool based on the bacterial CRISPR immune system, in which guideRNA (gRNA) recruits the Cas9 nuclease to the target locus in the genome through sequence complementarity and induces double-strand breaks (DSBs) [25–29]. These DSBs cause small insertions or deletions following non-homologous end-joining repair or can be utilized to introduce defined sequence modifications through a homology-dependent repair mechanism [25–29]. In the present study, we applied the CRISPR/Cas9 system to create a *MET* exon 14 deletion *in vitro* model, and the resulting phenotype, including its sensitivity to a *MET* inhibitor, was investigated.

2. Materials and methods

2.1. Database analysis

To analyze the prevalence of genomic alterations of the *MET* gene, the cBioPortal for Cancer Genomics database (<http://www.cbioportal.org/public-portal/>) was searched [30,31]. Both copy number variations and gene mutation data were analyzed across cancer types. In The Cancer Genome Atlas (TCGA) dataset (<http://cancergenome.nih.gov/>), several cancers were analyzed for *MET* splice site mutations.

2.2. Cell cultures and reagents

The HEK293 cell line (human embryonic kidney cell line) was maintained in DMEM medium (Nissui Pharmaceutical, Tokyo, Japan) supplemented with 10% FBS (GIBCO BRL, Grand Island, NY) in a humidified atmosphere of 5% CO₂ at 37 °C. The HEK293 cell line was obtained from ATCC and was authenticated using a short tandem repeat method. Crizotinib was purchased from Selleck Chemicals (Houston, TX). HGF was purchased from R&D Systems (Minneapolis, MN).

2.3. Plasmid construction and transfectants

pU6-gRNA/CMV-Cas9-GFP vectors including custom-designed gRNAs (gRNA-1 and gRNA-2) were purchased from Sigma-Aldrich (St. Louis, MO) (Supplementary Fig. S1). The vectors were transfected into HEK293 cells using FuGENE6 transfection reagent (Roche Diagnostics, Basel, Switzerland). After 48 h of transfection, GFP-positive cells were collected using flow cytometry (BD Biosciences, San Jose, CA) and a single clone was selected. After confirmation, the edited and unedited cell lines were designated as HEK293/Ex14Del-1, HEK293/Ex14Del-2, HEK293/Control-1, and HEK293/Control-2, respectively.

2.4. gRNA design

The gRNAs were designed by searching for “GG” or “CC” sequences (protospacer adjacent motif; PAM) near the target sites and were defined as NGG or the reverse complement sequence of CCN. The following gRNAs were used in this

study: gRNA-1, 5′-TGTTAAAGACGGCTATCATGGG-3′; gRNA-2, 5′-CCTATACATATACCTCAGTGGG-3′ (Fig. 1).

2.5. Sequencing

The PCR reactions were performed using TaKaRa ExTaq (TaKaRa, Otsu, Japan). The PCR products were then directly sequenced using the BigDye Terminator v3.1 sequencing kit (Applied Biosystems, Foster City, CA), as previously described [32]. The following primers were used: *MET* intron 13-F, 5′-GATTGCTGGTGTGTCTCAATATC-3′; *MET* intron 14-R, 5′-TGTCAAATACTTACTTGGCAGAGGTAAA-3′.

2.6. Analysis of *MET* exon 14 deletion

One microgram of total RNA from the cultured cell lines was converted to cDNA using the GeneAmp RNA-PCR kit (Applied Biosystems). The used primers were designed in *MET* exon 13 and *MET* exon 15 so as to interleave *MET* exon 14 as follows: *MET* exon 13-F, 5′-GGATTGATTGCTGGTGTGTCT-3′; and *MET* exon 15-R, 5′-GCACTTGTCGGCATGAACC-3′.

2.7. Real time reverse transcription PCR (RT-PCR)

Real time RT-PCR was performed using SYBR Premix Ex Taq and Thermal Cycler Dice (TaKaRa), as previously described [33]. Glyceraldehyde 3-phosphate dehydrogenase (*GAPD*, NM_002046) was used to normalize the expression levels in subsequent quantitative analyses. The experiment was performed in triplicate. To amplify the target genes encoding *MET*, the following primers were used: *MET* exon 11/12-F, 5′-GGGCAATGAAAATGTACTGGAA-3′; *MET* exon 11/12-R, 5′-ATTGGGGACCGTGCATAAAA-3′; *MET* exon 14/15-F, 5′-TGAGTACCGGAGACAGGTGCAG-3′; and *MET* exon 14/15-R, 5′-TAGCAGCTTCAACGGCAAAGTTC-3′.

2.8. Antibody

Rabbit antibodies specific for *MET*, phospho-*MET*, ERK1/2, phospho-ERK1/2, and β-actin were obtained from Cell Signaling (Beverly, MA).

2.9. Western blot analysis

A western blot analysis was performed as described previously [32]. Briefly, subconfluent cells were washed with cold phosphate-buffered saline (PBS) and harvested with Lysis A buffer containing 1% Triton X-100, 20 mM Tris–HCl (pH7.0), 5 mM EDTA, 50 mM sodium chloride, 10 mM sodium pyrophosphate, 50 mM sodium fluoride, 1 mM sodium orthovanadate, and the protease inhibitor mix Complete™ (Roche Diagnostics). Whole-cell lysates were separated using SDS-PAGE and were blotted onto a polyvinylidene fluoride membrane. After blocking with 3% bovine serum albumin in a TBS buffer (pH 8.0) with 0.1% Tween-20, the membrane was probed with the primary antibody. After rinsing twice with TBS buffer, the membrane was incubated with a horseradish peroxidase-conjugated secondary antibody and washed, followed by visualization using an ECL detection system and LAS-4000 (GE Healthcare, Buckinghamshire, United Kingdom).

2.10. Cellular growth assay

The cellular growth assay was performed using a 3, 4, 5-dimethyl-2H-tetrazolium bromide assay (MTT; Sigma-Aldrich), as described previously [34]. The experiment was performed in triplicate.

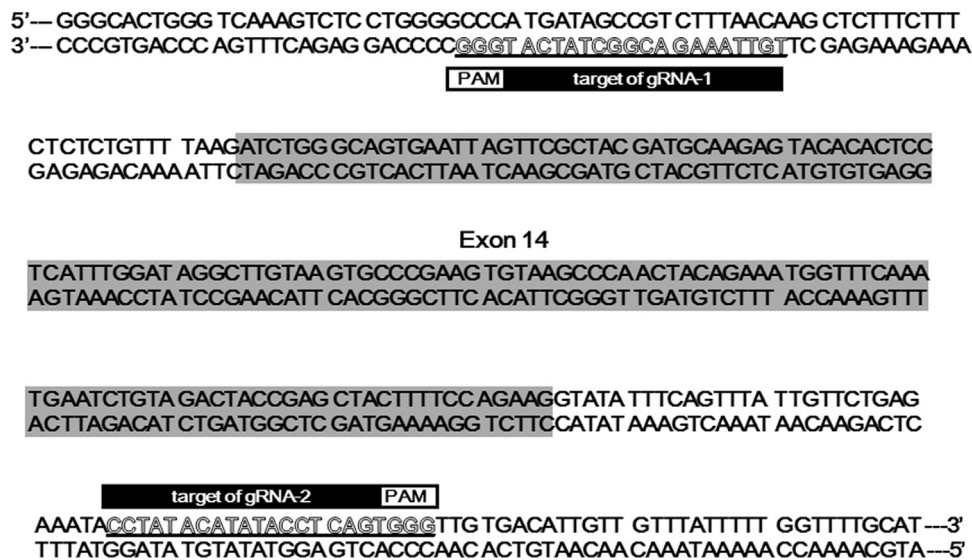


Fig. 1. A schematic illustration showing the locations of the gRNAs, along with the human *MET* locus. The bars and letters indicate the position of the gRNA targets with the protospacer adjacent motif (PAM) sequences. The gray halftones indicate *MET* exon 14.

2.11. Soft-agar assay

The soft-agar assay was performed as described previously [17]. Briefly, 20,000 HEK293 transfectant cells were suspended in 0.4% agarose with 10% FBS in DMEM and were then plated in a 6-well plate for 2 weeks.

2.12. In vitro growth inhibition assay

The growth-inhibitory effect of crizotinib was examined using an MTT assay, as described previously [32]. The experiment was performed in triplicate.

2.13. Statistical analysis

Continuous variables were analyzed using the Student *t*-test, and the results were expressed as the average and standard deviation (SD). The statistical analyses were two-tailed and were performed using Microsoft Excel (Microsoft, Redmond, WA). A *P* value of less than 0.05 was considered statistically significant.

3. Results

3.1. Frequency of *MET* exon 14 deletion in databases

We investigated the frequency of *MET* gene alterations in major cancers using the cBioPortal for Cancer Genomics database (<http://www.cbioportal.org/public-portal/>) (Supplementary Fig. S2). Furthermore, *MET* splicing site mutations (*MET* exon 14 deletions) were analyzed using the TCGA dataset (Table 1). These cancers were selected because some were reported to have a high frequency of *MET* alterations, some were common cancers, and the others were reported to have *MET* exon 14 deletions [17]. As shown in Table 1, lung adenocarcinoma had the highest incidence of *MET* exon 14 deletions, while the other cancers rarely carried such mutations. In the lung adenocarcinoma TCGA dataset, the *MET* exon 14 deletion was exclusive of other known driver gene alterations (*EGFR*, *KRAS*, *BRAF*, *HRAS*, *NRAS*, *MAP2K1*, *ALK*, *RET*, and *ROS1*). Approximately 10% of the samples without any of these alterations had the *MET* exon 14 deletion (10/101) [19].

3.2. CRISPR/Cas9 system induced deletions near the *MET* exon 14 splicing site

To create *MET* exon 14 deletions using the CRISPR/Cas9 system, two gRNAs were designed near the splicing site of *MET* exon 14 (gRNA-1 and gRNA-2) after considering the off-target effects (Fig. 1). After transfection into the HEK293 cell line, GFP-positive cells were collected using flow cytometry and single cell cloning was performed. Six clones were created for both transfectant cell lines. For each clone, the deletion of the splicing site of *MET* exon 14 was confirmed by direct sequencing (Fig. 2), and the confirmed clones were designated as HEK293/Ex14Del-1 and HEK293/Ex14Del-2, respectively. Clones in which no deletion of the splicing site was present were designated as HEK293/Control-1 and HEK293/Control-2, respectively.

In the HEK293/Ex14Del-1 cell line, a 183-bp region around the splicing site of *MET* exon 14 was deleted in one allele, and a 7-bp region was deleted in another allele (Fig. 2). In the HEK293/Ex14Del-2 cell line, a 167-bp region around the splicing site of *MET* exon 14 was deleted in one allele, and a 2-bp region was deleted in another allele (Fig. 2).

3.3. Creation of *MET* exon 14 deletion using the CRISPR/Cas9 system

To confirm the deletion of *MET* exon 14, primers that were interleaved with *MET* exon 14 were designed for exon 13 (*MET* exon 13-F) and exon 15 (*MET* exon 15-R) (Fig. 3A). The wild-type allele was amplified to 277 bp, and the deleted allele was amplified to 136 bp. The 277-bp band was only amplified in the HEK293, HEK293/Control-1, HEK293/Control-2, A549, and EBC-1 cell lines, whereas both bands were amplified in the HEK293/Ex14Del-1 and HEK293/Ex14Del-2 cell lines; these two bands were concentrated equally (Fig. 3A).

Next, to quantitate the expressions, real time RT-PCR was performed. The product that was amplified by the *MET* exon 11/12 primers represented the expression of whole *MET* mRNA, while the product that was amplified by the *MET* exon 14/15 primers represented the expression of *MET* mRNA with exon 14. The expression of *MET* mRNA with exon 14 was about half of that of whole *MET* mRNA in the HEK293/Ex14Del-1 and HEK293/Ex14Del-2 cell lines (Fig. 3B). These findings indicated that the *MET* exon 14 deletion

Table 1
MET gene alterations in TCGA.

Dataset	Number	Mutation	Amp	Del	Multiple	Total	Exon 14 deletion
Lung Adenocarcinoma	230	18 (7.8%)	7 (3.0%)	1 (0.4%)	1 (0.4%)	27 (11.7%)	10 (4.3%)
Lung Squamous Cell Carcinoma	178	2 (1.1%)	2 (1.1%)	0 (0.0%)	0 (0.0%)	4 (2.2%)	0 (0.0%)
Esophageal Carcinoma	184	NA ^a	7 (3.8%)	3 (1.6%)	0 (0.0%)	10 (5.4%)	0 (0.0%)
Stomach Adenocarcinoma	287	5 (1.7%)	11 (3.8%)	0 (0.0%)	1 (0.3%)	17 (5.9%)	0 (0.0%)
Colorectal Adenocarcinoma	212	4 (1.9%)	1 (0.5%)	1 (0.5%)	0 (0.0%)	6 (2.8%)	0 (0.0%)
Liver Hepatocellular Carcinoma	193	0 (0.0%)	6 (3.1%)	0 (0.0%)	0 (0.0%)	6 (3.1%)	0 (0.0%)
Renal Papillary Cell Carcinoma	161	15 (9.3%)	3 (1.9%)	0 (0.0%)	0 (0.0%)	18 (11.2%)	0 (0.0%)
Renal Clear Cell Carcinoma	415	2 (0.5%)	5 (1.2%)	0 (0.0%)	0 (0.0%)	7 (1.7%)	0 (0.0%)
Renal Chromophobe Cell Carcinoma	65	0 (0.0%)	1 (1.5%)	0 (0.0%)	0 (0.0%)	1 (1.5%)	0 (0.0%)
Bladder Urothelial Carcinoma	127	4 (3.1%)	0 (0.0%)	0 (0.0%)	0 (0.0%)	4 (3.1%)	0 (0.0%)
Prostate Adenocarcinoma	333	3 (0.9%)	3 (0.9%)	3 (0.9%)	0 (0.0%)	9 (2.7%)	0 (0.0%)
Ovarian Serous Cystadenocarcinoma	316	4 (1.3%)	5 (1.6%)	1 (0.3%)	0 (0.0%)	10 (3.2%)	0 (0.0%)
Uterine Corpus Endometrioid Carcinoma	240	13 (5.4%)	1 (0.4%)	0 (0.0%)	0 (0.0%)	14 (5.8%)	0 (0.0%)
Breast Carcinoma	482	2 (0.4%)	0 (0.0%)	0 (0.0%)	0 (0.0%)	2 (0.4%)	0 (0.0%)
Melanoma	278	18 (6.5%)	9 (3.2%)	0 (0.0%)	2 (0.7%)	29 (10.4%)	0 (0.0%)
Glioma	286	2 (0.7%)	8 (2.8%)	0 (0.0%)	1 (0.3%)	11 (3.8%)	1 (0.3%)
Glioblastoma	281	1 (0.4%)	7 (2.5%)	0 (0.0%)	0 (0.0%)	8 (2.8%)	0 (0.0%)
Adenocortical Carcinoma	88	0 (0.0%)	0 (0.0%)	1 (1.1%)	0 (0.0%)	1 (1.1%)	0 (0.0%)
Sarcoma	257	0 (0.0%)	7 (2.7%)	0 (0.0%)	0 (0.0%)	7 (2.7%)	0 (0.0%)

Abbreviations: Amp, amplification; Del, deletion.
^a Mutation data is not available.

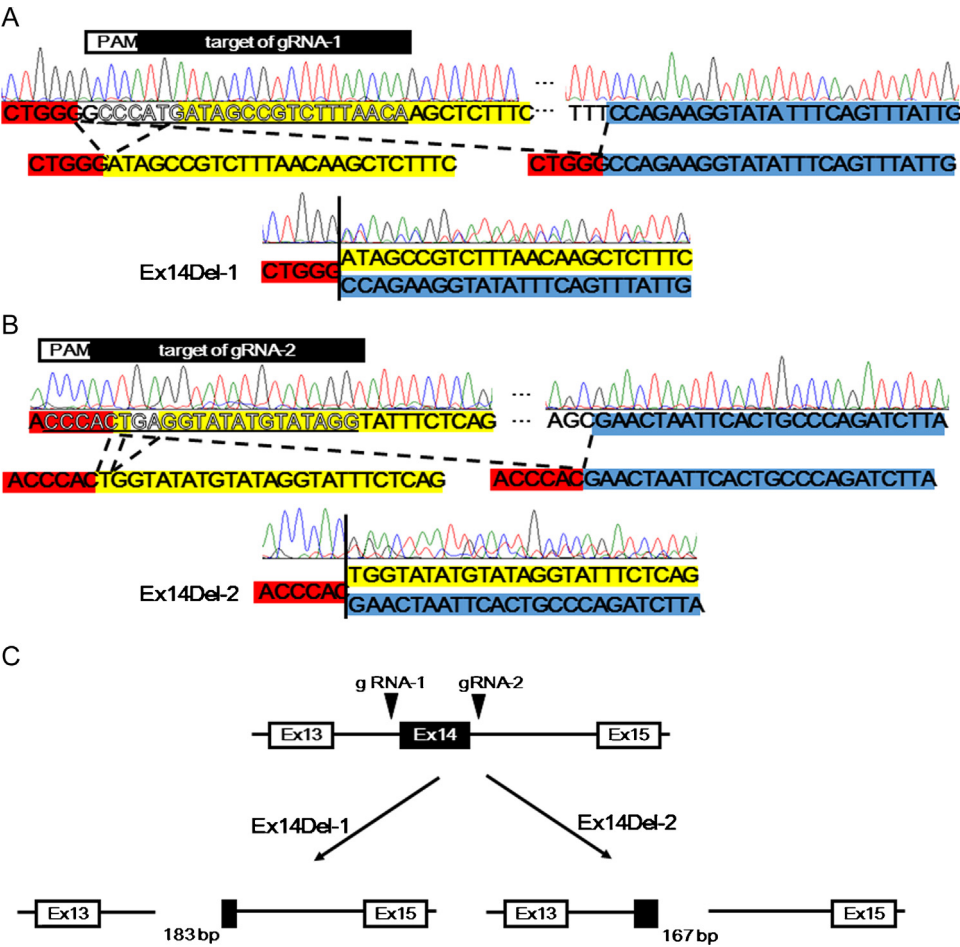


Fig. 2. Results of the sequence analysis of the *MET* exon 14 locus. The *MET* exon 14 locus around the gRNAs target site was amplified and directly sequenced. (A) HEK293/Ex14Del-1 cell line: a 183-bp region around the splicing site of *MET* exon 14 (gRNA-1 target site) was deleted in one allele, and a 7-bp region was deleted in another allele. (B) HEK293/Ex14Del-2 cell line: a 167-bp region around the splicing site of *MET* exon 14 (gRNA-2 target site) was deleted in one allele, and a 2-bp region was deleted in another allele. (C) Diagram of the *MET* gene in the transfectant HEK293 cell lines.

was created by the CRISPR/Cas9 system and that wild-type *MET* mRNA was expressed at a level similar to that of exon 14-deleted *MET* mRNA in these cell lines. A western blot analysis revealed that the HEK293/Ex14Del cell lines exhibited bands that were slightly smaller than the wild-type *MET* band, indicating that the protein of exon 14-deleted *MET* was expressed in these cell lines. In addition, the bands of exon 14-deleted *MET* were more concentrated than the wild-type band, suggesting that the protein expression of exon

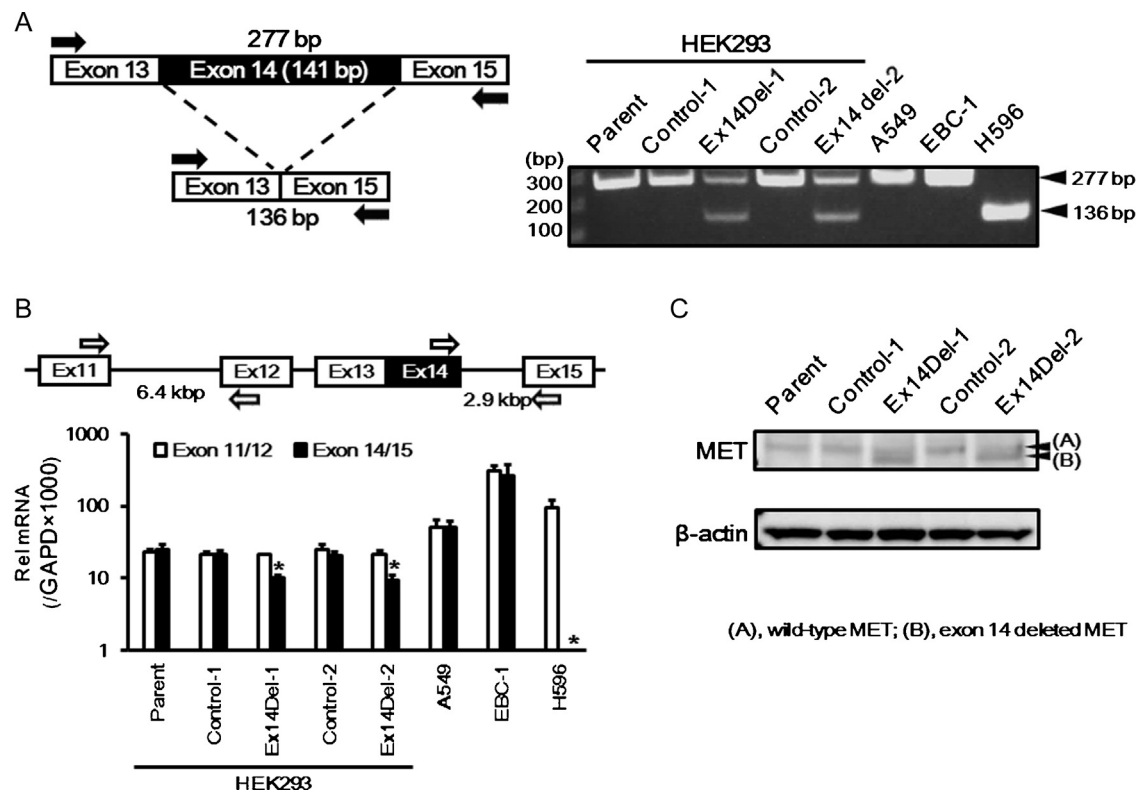


Fig. 3. Expression of exon 14-deleted MET. **(A)** PCR products amplified from cDNA. To confirm the deletion of MET exon 14, primers that interleaved *MET* exon 14 were designed for exon 13 and 15. The wild-type allele was amplified to 277 bp, and the deleted allele was amplified to 136 bp. The 277-bp band was only amplified in the HEK293, HEK293/Control-1, HEK293/Control-2, A549, and EBC-1 cell lines, whereas both bands were amplified in the HEK293/Ex14Del-1 and HEK293/Ex14Del-2 cell lines. The two bands were equally concentrated. The H596 cell line, which only expressed exon 14-deleted MET, was used as a positive control. **(B)** Real time RT-PCR. To quantitate the expression, real time RT-PCR was performed. The experiment was performed in triplicate. The product amplified by the *MET* exon 11/12 primers represented the expression of whole *MET* mRNA, whereas the product amplified by the *MET* exon 14/15 primers represented the expression of *MET* mRNA with exon 14. The expression of *MET* mRNA with exon 14 was about half of the expression of whole *MET* mRNA in the HEK293/Ex14Del-1 and HEK293/Ex14Del-2 cell lines. The expressions of whole *MET* mRNA in the HEK293, HEK293/Control-1, HEK293/Control-2, A549, and EBC-1 cell lines were similar to those of *MET* mRNA with exon 14. In contrast, the H596 cell line had no expression of *MET* mRNA with exon 14. Column, mean of independent triplicate experiments; error bars, SD; *, $P < 0.05$. **(C)** Western blot analysis. The protein expressions were evaluated using a western blot analysis. The (b) bands, which were slightly smaller than the wild-type MET (a) bands, were observed in the HEK293/Ex14Del-1 and HEK293/Ex14Del-2 cell lines. Furthermore, these (b) bands were more concentrated than the wild-type MET (a) bands in these cell lines. β-actin was used as an internal control.

14-deleted MET was higher than that of wild-type MET, despite the similar mRNA expression levels (Fig. 3C).

3.4. MET exon 14 deletion enhanced cellular growth and colony formation

To evaluate the role of exon 14-deleted MET, cellular growth and soft agar assays were performed. The cellular growth of the HEK293/Ex14Del cell lines was enhanced, compared with that of the controls (Fig. 4A). Furthermore, the colony formation of the HEK293/Ex14Del cell lines was also enhanced (Fig. 4B). The exon 14-deleted MET was slightly more phosphorylated than wild-type MET even without HGF stimulation. In addition, as described in a previous study [16], the phosphorylation of MET was prolonged by HGF stimulation in the HEK293/Ex14Del cell lines, resulting in the prolonged phosphorylation of ERK1/2. Furthermore, along with the protein expression of MET, the phosphorylation levels were higher for exon 14-deleted MET than for the wild-type MET (Fig. 4C).

3.5. MET exon 14 deletion enhanced sensitivity to a MET inhibitor

Next, to investigate the influence of the *MET* exon 14 deletion on MET inhibitor sensitivity, a growth inhibition assay for crizotinib was performed using an MTT assay. The HEK293/Ex14Del cell lines were more sensitive to crizotinib than the controls (Fig. 5A). The 50% inhibitory concentrations (IC_{50}) of each of the cell lines

to crizotinib were Ex14Del-1, 0.49 μ M vs. Control-1, 2.23 μ M and MET14Del-2, 0.35 μ M vs. Control-2, 1.79 μ M, respectively. The enhanced phosphorylation of MET and ERK1/2 was greatly inhibited by crizotinib in the HEK293/Ex14Del cell lines, whereas the phosphorylation was slightly inhibited in the controls (Fig. 5B), possibly explaining the reason for the higher sensitivities to the MET inhibitor in the HEK293/Ex14Del cell lines.

4. Discussion

The RNA-guided enzyme Cas9, which originated from the CRISPR/Cas adaptive bacterial immune system, is transforming biology by providing a genome-engineering tool. The CRISPR/Cas9 system has been used to introduce defined genetic modifications to both cultured cell systems and in vivo systems. We easily and rapidly created cell lines with an *MET* exon 14 deletion using this system. Our experiments using these cell lines indicated that *MET* exon 14 deletions enhanced cellular growth, colony formation, and MET inhibitor sensitivity. To the best of our knowledge, this is the first study to create an in vitro model of *MET* exon 14 deletion using the CRISPR/Cas9 system.

In 2012, Jinek et al. demonstrated, for the first time, that the CRISPR/Cas9 system is an efficient tool for editing the genomes of human cells [29]. The CRISPR-associated protein Cas9 is an endonuclease that uses a guide sequence within an RNA duplex, tracrRNA:crRNA, to form base pairs with DNA target sequences,

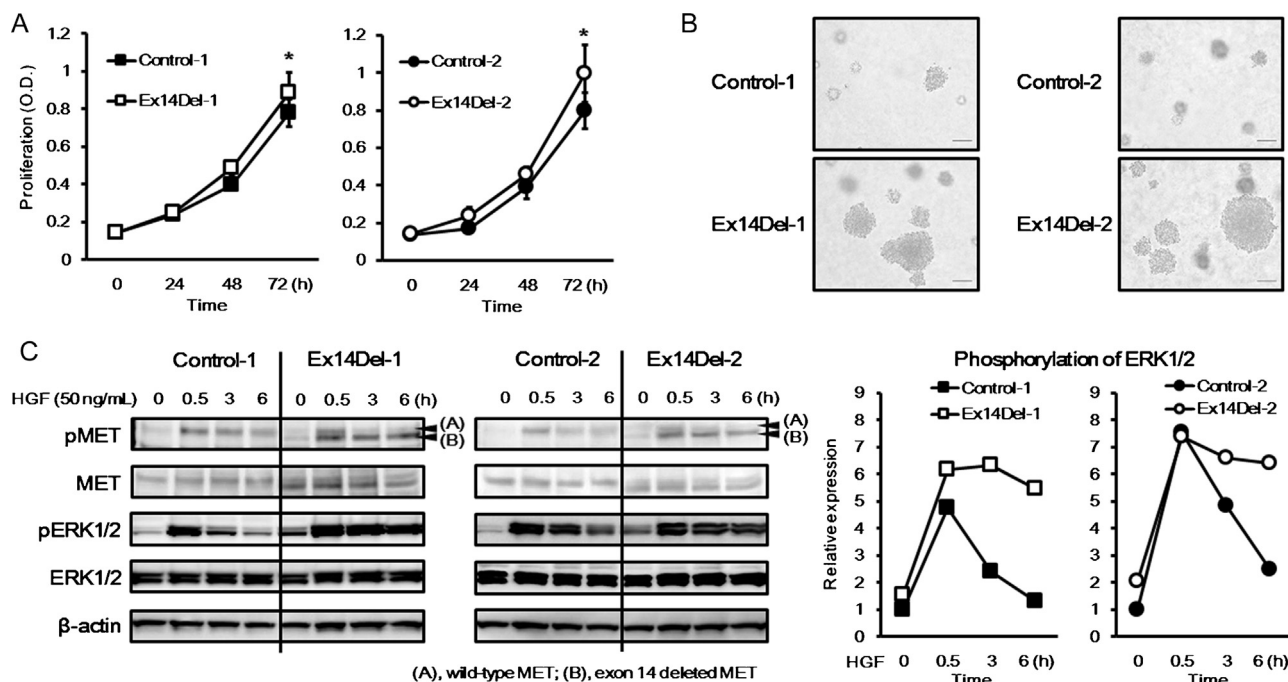


Fig. 4. Cellular growth and colony formation of the transfectant cell lines. (A) Cellular growth of each transfectant cell line. Cellular growth was evaluated using an MTT assay, and the experiment was performed in triplicate. The cellular growth of both *MET* exon 14-deleted cell lines was enhanced, compared with the controls. Line, mean of independent triplicate experiments; error bars, SD; *, $P < 0.05$. (B) Colony formation of each transfectant cell line. Colony formation was evaluated using a soft-agar assay. The colony formation of the HEK293/Ex14Del cell lines was enhanced, compared with the controls. Scale bar, 100 μm . (C) Western blot analysis. Without HGF stimulation (0 h), the phosphorylation levels of MET and ERK1/2 were slightly increased in the *MET* exon 14-deleted cell lines, compared with the controls. In addition, the phosphorylation levels of MET and ERK1/2 were maintained after HGF stimulation in the *MET* exon 14-deleted cell lines, whereas the phosphorylation levels decreased 3 or 6 h after stimulation in the controls. In the *MET* exon 14-deleted cell lines, the phosphorylation level of exon 14-deleted MET (b) was higher and more maintained than that of wild-type MET (a). The relative expressions of phosphorylated ERK1/2 were graphed to show the maintenance of ERK1/2 phosphorylation in the *MET* exon 14-deleted cell lines, compared with that in the controls. β -actin was used as an internal control.

enabling Cas9 to introduce a site-specific DSB into the DNA. The CRISPR system from *S. pyogenes* has been adapted for inducing sequence-specific DSBs and targeted genome editing. Twenty nucleotides at the 5' end of the gRNA (corresponding to the protospacer portion of the crRNA) direct Cas9 to a specific target DNA site using standard RNA-DNA complementarity base-pairing rules. These target sites must lie immediately 5' of a PAM sequence that matches the canonical form 5'-NGG. Thus, with this system, Cas9 nuclease activity can be directed to any DNA sequence with the form of N20-NGG simply by altering the first 20 nucleotides of the gRNA to correspond to the target DNA sequence [25–28]. In the present study, two gRNA sequences were designed around the human *MET* exon 14 splicing site after considering their off-target effects. Both of these sequences easily and rapidly deleted *MET* exon 14, suggesting that this system may be useful for such experiments.

Deletions within the juxtamembrane domain play an important role in the activation of RTKs by altering receptor conformation and the activation of the kinase domain [35]. A previous report identified *MET* activation through a somatic mutation-driven exon 14 deletion that inhibited *MET* down-regulation and showed that the loss of Cbl binding to the *MET* exon 14 deletion affected receptor ubiquitination and down-regulation, leading to prolonged *MET* activation and oncogenesis [16]. Our *in vitro* model created using the CRISPR/Cas9 system produced similar results, that is, a higher *MET* protein expression level, enhanced *MET* phosphorylation, and prolonged *MET* activation by HGF. In addition, we directly compared cellular growth and sensitivity to crizotinib using cell lines that were created from the same HEK293 cell line using the CRISPR/Cas9 system, showing that cellular growth, colony formation, and sensitivity were enhanced by *MET* exon 14 deletion. Although enhanced cellular growth, colony formation, and sensitivity as a result of *MET* exon 14 deletion have been suggested in a

previous study, a direct comparison was not possible because several different cell lines were used [16]. A recent study also revealed similar results, but a mouse *MET* exon 15 deletion-overexpressed NIH3T3 mouse cell line was used in the experiments [17]. Therefore, our experiments showed enhanced cellular growth, colony formation, and sensitivity in a more direct manner using a human cell line edited using the CRISPR/Cas9 system for the first time.

In the database analysis, the *MET* exon 14 deletion was found most frequently in lung cancer, especially lung adenocarcinoma, and other cancers rarely carried this mutation. One gastric cancer cell line has been reported to have a *MET* exon 14 deletion, but none of the gastric cancer samples in the TCGA dataset exhibited such a deletion [36]. In lung adenocarcinoma, this mutation was exclusive with other lung cancer driver gene alterations, and approximately 10% of patients with wild-type *EGFR*, *RAS*, *RAF*, *ALK*, *RET*, and *ROS1* may carry the *MET* exon 14 deletion [19]. This frequency is considerably high, and the development of *MET*-targeted therapy for lung adenocarcinoma with *MET* exon 14 deletion should be considered.

Because the CRISPR/Cas9 system is a novel technology, unknown effects, including off-target effects, may exist. In particular, cancer cell lines can have numerous somatic mutations that can induce unexpected off-target effects. We were unable to create the *MET* exon 14 deletion in any NSCLC cell lines. Consequently, we did not use cancer cell lines in the present study but instead used the HEK293 cell line. In addition, we created two cell lines using two different gRNAs sequences and obtained the same results. Our experiments using this system directly showed enhanced cellular growth, colony formation, and *MET* inhibitor sensitivity. These findings suggest that this system can be useful for similar experiments, and the presently obtained experimental findings strongly encourage the development of *MET*-targeted therapy against cancers with the *MET* exon 14 deletion.

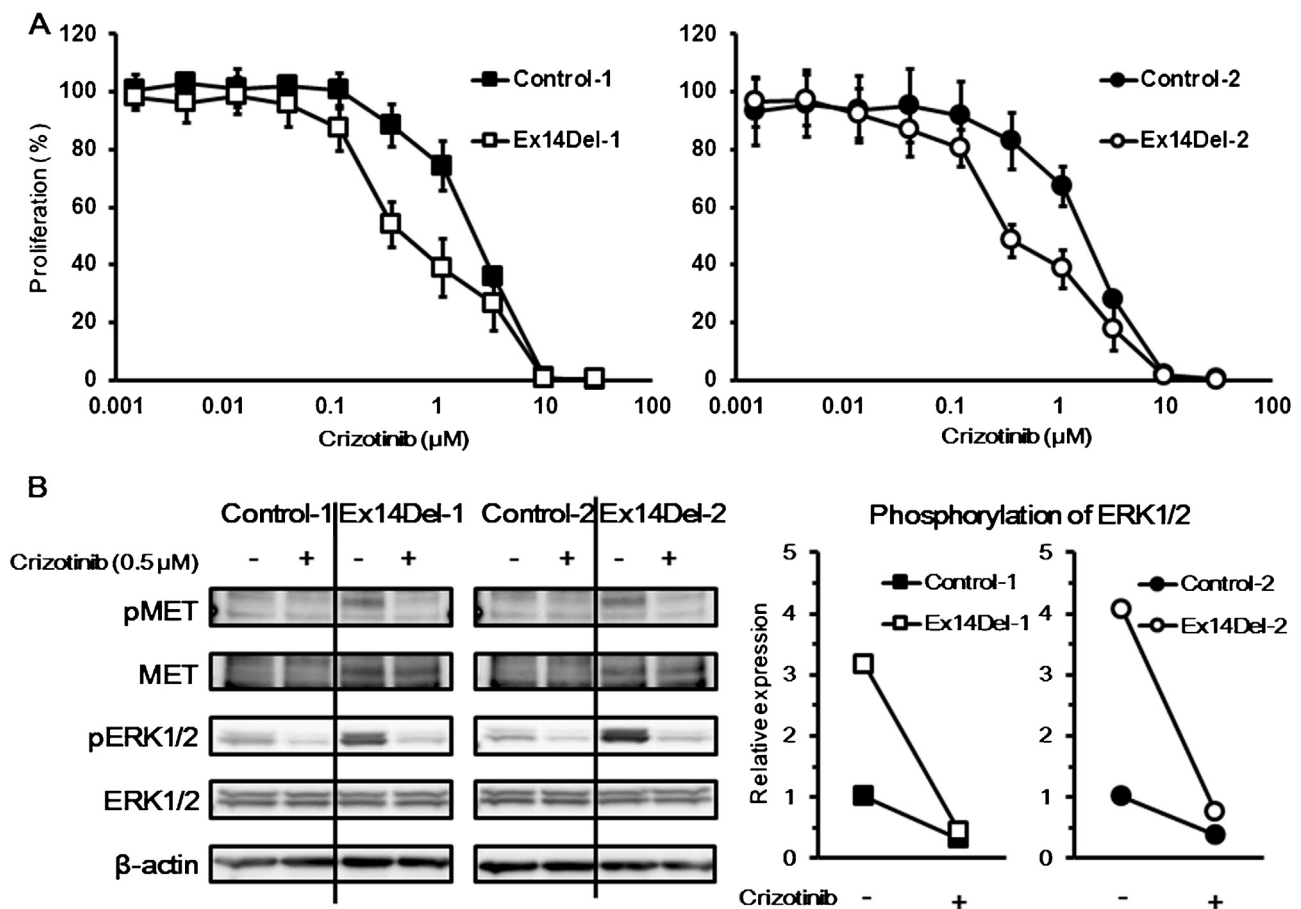


Fig. 5. Sensitivity to crizotinib. (A) Growth inhibition assay of each transfectant cell line. The growth inhibition assay was performed using an MTT assay, and the experiment was performed in triplicate. Both *MET* exon 14-deleted cell lines were more sensitive to crizotinib than the controls. Line, mean of independent triplicate experiments; error bars, SD. (B) Western blot analysis. Cells were exposed to HGF (50 ng/mL) with or without crizotinib (0.5 μM) 6 h before sample collection. The HGF-induced increase in the phosphorylation of MET and ERK1/2 was greatly reduced by crizotinib in the *MET* exon 14-deleted cell lines. In the controls, however, the phosphorylation was decreased without crizotinib and was slightly reduced by crizotinib. The relative expressions of phosphorylated ERK1/2 were graphed to show the marked reduction of ERK1/2 phosphorylation in the *MET* exon 14-deleted cell lines, compared with that in the controls. β-actin was used as an internal control.

Conflict of interest

T. Mitsudomi has received honoraria from Pfizer Pharmaceuticals; the other authors do not have any potential conflicts of interest to report.

Acknowledgments

We thank Mr. Shinji Kurashimo, Ms. Tomoko Kitayama, and Ms. Ayaka Kurumatani for their technical assistance. This study was supported by Grants-in Aid from the Japan Society for Promotion of Science Fellows, Takeda Science Foundation, and Uehara Memorial Foundation.

Appendix A. Supplementary data

Supplementary data associated with this article can be found, in the online version, at <http://dx.doi.org/10.1016/j.lungcan.2015.10.020>.

References

- [1] R. Siegel, J. Ma, Z. Zou, A. Jemal, Cancer statistics, 2014, *CA Cancer J Clin* 64 (1) (2014) 9–29, <http://dx.doi.org/10.3322/caac.21208>, PubMed PMID: 24399786.
- [2] J.G. Paez, P.A. Janne, J.C. Lee, S. Tracy, H. Greulich, S. Gabriel, et al., EGFR mutations in lung cancer: correlation with clinical response to gefitinib therapy, *Science* 304 (5676) (2004) 1497–1500, <http://dx.doi.org/10.1126/science.1099314>, Epub 2004/05/01, PubMed PMID: 15118125.
- [3] T.J. Lynch, D.W. Bell, R. Sordella, S. Gurubhagavatula, R.A. Okimoto, B.W. Brannigan, et al., Activating mutations in the epidermal growth factor receptor underlying responsiveness of non-small-cell lung cancer to gefitinib, *N. Engl. J. Med.* 350 (21) (2004) 2129–2139, <http://dx.doi.org/10.1056/NEJMoa040938>, Epub 2004/05/01, PubMed PMID: 15118073.
- [4] W. Pao, V. Miller, M. Zakowski, J. Doherty, K. Politi, I. Sarkaria, et al., EGF receptor gene mutations are common in lung cancers from never smokers and are associated with sensitivity of tumors to gefitinib and erlotinib, *Proc. Natl. Acad. Sci. U. S. A.* 101 (36) (2004) 13306–13311, <http://dx.doi.org/10.1073/pnas.0405220101>, PubMed PMID: 15329413; PubMed Central PMCID: PMC156528.
- [5] T.S. Mok, Y.L. Wu, S. Thongprasert, C.H. Yang, D.T. Chu, N. Saijo, et al., Gefitinib or carboplatin-paclitaxel in pulmonary adenocarcinoma, *N. Engl. J. Med.* 361 (10) (2009) 947–957, <http://dx.doi.org/10.1056/NEJMoa0810699>, Epub 2009/08/21, PubMed PMID: 19692680.
- [6] T. Mitsudomi, S. Morita, Y. Yatabe, S. Negoro, I. Okamoto, J. Tsurutani, et al., Gefitinib versus cisplatin plus docetaxel in patients with non-small-cell lung cancer harbouring mutations of the epidermal growth factor receptor (WJTOG3405): an open label, randomised phase 3 trial, *Lancet Oncol.* 11 (2) (2010) 121–128, [http://dx.doi.org/10.1016/S1470-2045\(09\)70364-x](http://dx.doi.org/10.1016/S1470-2045(09)70364-x), Epub 2009/12/22, PubMed PMID: 20022809.
- [7] M. Maemondo, A. Inoue, K. Kobayashi, S. Sugawara, S. Oizumi, H. Isobe, et al., Gefitinib or chemotherapy for non-small-cell lung cancer with mutated EGFR, *N Engl J Med.* 362 (25) (2010) 2380–2388, <http://dx.doi.org/10.1056/NEJMoa0909530>, Epub 2010/06/25, PubMed PMID: 20573926.
- [8] W. Pao, N. Girard, New driver mutations in non-small-cell lung cancer, *Lancet Oncol.* 12 (2) (2011) 175–180, [http://dx.doi.org/10.1016/S1470-2045\(10\)70087-5](http://dx.doi.org/10.1016/S1470-2045(10)70087-5), PubMed PMID: 21277552.
- [9] C.S. Cooper, M. Park, D.G. Blair, M.A. Tainsky, K. Huebner, C.M. Croce, et al., Molecular cloning of a new transforming gene from a chemically transformed human cell line, *Nature* 311 (5981) (1984) 29–33, PubMed PMID: 6590967.

- [10] L. Naldini, E. Vigna, R.P. Narsimhan, G. Gaudino, R. Zarnegar, G.K. Michalopoulos, et al., Hepatocyte growth factor (HGF) stimulates the tyrosine kinase activity of the receptor encoded by the proto-oncogene c-MET, *Oncogene* 6 (4) (1991) 501–504, PubMed PMID: 1827664.
- [11] L. Trusolino, A. Bertotti, P.M. Comoglio, MET signalling: principles and functions in development, organ regeneration and cancer, *Nat. Rev. Mol. Cell Biol.* 11 (12) (2010) 834–848, <http://dx.doi.org/10.1038/nrm3012>, PubMed PMID: 21102609.
- [12] R. Califano, A. Abidin, N.U. Tariq, P. Economopoulou, G. Metro, G. Mountzios, Beyond EGFR and ALK inhibition: unravelling and exploiting novel genetic alterations in advanced non small-cell lung cancer, *Cancer Treat. Rev.* 41 (5) (2015) 401–411, <http://dx.doi.org/10.1016/j.ctrv.2015.03.009>, PubMed PMID: 25842168.
- [13] A. Li, H.F. Gao, Y.L. Wu, Targeting the MET pathway for potential treatment of NSCLC, *Expert Opin. Ther. Targets* 19 (5) (2015) 663–674, <http://dx.doi.org/10.1517/14728222.2014.995093>, PubMed PMID: 25532429.
- [14] S.P. Hack, J.M. Bruey, H. Koeppen, HGF/MET-directed therapeutics in gastroesophageal cancer: a review of clinical and biomarker development, *Oncotarget* 5 (10) (2014) 2866–2880, PubMed PMID: 24930887; PubMed Central PMCID: PMC4021777.
- [15] E. Gherardi, W. Birchmeier, C. Birchmeier, G. Vande Woude, Targeting MET in cancer: rationale and progress, *Nat. Rev. Cancer* 12 (2) (2012) 89–103, <http://dx.doi.org/10.1038/nrc3205>, PubMed PMID: 22270953.
- [16] M. Kong-Beltran, S. Seshagiri, J. Zha, W. Zhu, K. Bhawe, N. Mendoza, et al., Somatic mutations lead to an oncogenic deletion of met in lung cancer, *Cancer Res.* 66 (1) (2006) 283–289, <http://dx.doi.org/10.1158/0008-5472.CAN-05-2749>, PubMed PMID: 16397241.
- [17] G.M. Frampton, S.M. Ali, M. Rosenzweig, J. Chmielecki, X. Lu, T.M. Bauer, et al., Activation of MET via diverse exon 14 splicing alterations occurs in multiple tumor types and confers clinical sensitivity to MET inhibitors, *Cancer Discov.* (2015), <http://dx.doi.org/10.1158/2159-8290>, CD-15-0285. PubMed PMID: 25971938.
- [18] R. Onozato, T. Kosaka, H. Kuwano, Y. Sekido, Y. Yatabe, T. Mitsudomi, Activation of MET by gene amplification or by splice mutations deleting the juxtamembrane domain in primary resected lung cancers, *J. Thorac. Oncol.* 4 (1) (2009) 5–11, <http://dx.doi.org/10.1097/JTO.0b013e3181913e0e>, PubMed PMID: 19096300.
- [19] Network CGAR, Comprehensive molecular profiling of lung adenocarcinoma, *Nature* 511 (7511) (2014) 543–550, <http://dx.doi.org/10.1038/nature13385>, PubMed PMID: 25079552; PubMed Central PMCID: PMC4231481.
- [20] E.L. Kwak, Y.J. Bang, D.R. Camidge, A.T. Shaw, B. Solomon, R.G. Maki, et al., Anaplastic lymphoma kinase inhibition in non-small-cell lung cancer, *N. Engl. J. Med.* 363 (18) (2010) 1693–1703, <http://dx.doi.org/10.1056/NEJMoa1006448>, PubMed PMID: 20979469; PubMed Central PMCID: PMC3014291.
- [21] A.T. Shaw, B.J. Solomon, Crizotinib in ROS1-rearranged non-small-cell lung cancer, *N. Engl. J. Med.* 372 (7) (2015) 683–684, <http://dx.doi.org/10.1056/NEJMc1415359>, PubMed PMID: 25671264.
- [22] J.J. Cui, M. Tran-Dubé, H. Shen, M. Nambu, P.P. Kung, M. Pairish, et al., Structure based drug design of crizotinib (PF-02341066), a potent and selective dual inhibitor of mesenchymal-epithelial transition factor (c-MET) kinase and anaplastic lymphoma kinase (ALK), *J. Med. Chem.* 54 (18) (2011) 6342–6363, <http://dx.doi.org/10.1021/jm2007613>, PubMed PMID: 21812414.
- [23] S. Oxnard, E.K. Elkin, J.L. Sullivan, D.A. Carter, Response to Crizotinib in a Patient With Lung Adenocarcinoma Harboring a MET Splice Site Mutation, *Clin Lung Cancer* (2015), <http://dx.doi.org/10.1016/j.clcc.2015.01.009>, PubMed PMID: 25769807.
- [24] P.K. Paik, A. Drilon, H. Yu, N. Rekhtman, M.S. Ginsberg, L. Borsu, et al., Response to MET inhibitors in patients with stage IV lung adenocarcinomas harboring MET mutations causing exon 14 skipping, *Cancer Discov.* (2015), <http://dx.doi.org/10.1158/2159-8290>, CD-14-1467. PubMed PMID: 25971939.
- [25] P. Mali, L. Yang, K.M. Esvelt, J. Aach, M. Guell, J.E. DiCarlo, et al., RNA-guided human genome engineering via Cas9, *Science* 339 (6121) (2013) 823–826, <http://dx.doi.org/10.1126/science.1232033>, PubMed PMID: 23287722; PubMed Central PMCID: PMC3712628.
- [26] J.A. Doudna, E. Charpentier, Genome editing, The new frontier of genome engineering with CRISPR-Cas9, *Science* 346 (6213) (2014) 1258096, <http://dx.doi.org/10.1126/science.1258096>, PubMed PMID: 25430774.
- [27] J.D. Sander, J.K. Joung, CRISPR-Cas systems for editing, regulating and targeting genomes, *Nat. Biotechnol.* 32 (4) (2014) 347–355, <http://dx.doi.org/10.1038/nbt.2842>, PubMed PMID: 24584096; PubMed Central PMCID: PMC4022601.
- [28] L. Cong, F.A. Ran, D. Cox, S. Lin, R. Barretto, N. Habib, et al., Multiplex genome engineering using CRISPR/Cas systems, *Science* 339 (6121) (2013) 819–823, <http://dx.doi.org/10.1126/science.1231143>, PubMed PMID: 23287718; PubMed Central PMCID: PMC3795411.
- [29] M. Jinek, K. Chylinski, I. Fonfara, M. Hauer, J.A. Doudna, E. Charpentier, A programmable dual-RNA-guided DNA endonuclease in adaptive bacterial immunity, *Science* 337 (6096) (2012) 816–821, <http://dx.doi.org/10.1126/science.1225829>, PubMed PMID: 22745249.
- [30] E. Cerami, J. Gao, U. Dogrusoz, B.E. Gross, S.O. Sumer, B.A. Aksoy, et al., The cBio cancer genomics portal: an open platform for exploring multidimensional cancer genomics data, *Cancer Discov.* 2 (5) (2012) 401–404, <http://dx.doi.org/10.1158/2159-8290>, CD-12-0095. PubMed PMID: 22588877; PubMed Central PMCID: PMC3956037.
- [31] J. Gao, B.A. Aksoy, U. Dogrusoz, G. Dresdner, B. Gross, S.O. Sumer, et al., Integrative analysis of complex cancer genomics and clinical profiles using the cBioPortal, *Sci. Signal.* 6 (269) (2013) p11, <http://dx.doi.org/10.1126/scisignal.2004088>, PubMed PMID: 23550210; PubMed Central PMCID: PMC4160307.
- [32] S. Sogabe, Y. Togashi, H. Kato, A. Kogita, T. Mizukami, Y. Sakamoto, et al., MEK Inhibitor for Gastric Cancer with MEK1 Gene Mutations, *Mol. Cancer Ther.* 13 (12) (2014) 3098–3106, <http://dx.doi.org/10.1158/1535-7163.MCT-14-0429>, PubMed PMID: 25253779.
- [33] K. Matsumoto, T. Arao, T. Hamaguchi, Y. Shimada, K. Kato, I. Oda, et al., FGFR2 gene amplification and clinicopathological features in gastric cancer, *Br. J. Cancer* 106 (4) (2012) 727–732, <http://dx.doi.org/10.1038/bjc.2011.603>, PubMed PMID: 22240789; PubMed Central PMCID: PMC3322955.
- [34] Y. Togashi, A. Kogita, H. Sakamoto, H. Hayashi, M. Terashima, M.A. de Velasco, et al., Activin signal promotes cancer progression and is involved in cachexia in a subset of pancreatic cancer, *Cancer Lett.* 356 (2 Pt. B) (2015) 819–827, <http://dx.doi.org/10.1016/j.canlet.2014.10.037>, PubMed PMID: 25449777.
- [35] S.R. Hubbard, Juxtamembrane autoinhibition in receptor tyrosine kinases, *Nat. Rev. Mol. Cell Biol.* 5 (6) (2004) 464–471, <http://dx.doi.org/10.1038/nrm1399>, PubMed PMID: 15173825.
- [36] Y. Asaoka, M. Tada, T. Ikenoue, M. Seto, M. Imai, K. Miyabayashi, et al., Gastric cancer cell line Hs746T harbors a splice site mutation of c-Met causing juxtamembrane domain deletion, *Biochem. Biophys. Res. Commun.* 394 (4) (2010) 1042–1046, <http://dx.doi.org/10.1016/j.bbrc.2010.03.120>, PubMed PMID: 20331976.